PHYSICAL REVIEW A **69**, 051401(R) (2004)

Polarization effects in two-photon nonresonant ionization of argon with extreme-ultraviolet and infrared femtosecond pulses

P. O'Keeffe,[1] R. López-Martens,[2] J. Mauritsson,[2] A. Johansson,[2] A. L'Huillier,[2]
V. Véniard,[3] R. Taïeb,[3] A. Maquet,[3] and M. Meyer[1,4]
[1]*LURE, Centre Universitaire Paris-Sud, Bâtiment 209D, F-91898 Orsay Cedex, France*
[2]*Department of Physics, Lund Institute of Technology, P.O. Box 118, S-22100 Lund, Sweden*
[3]*LCP-MR, Université Pierre et Marie Curie, 11 Rue Pierre et Marie Curie, F-75231 Paris Cedex 05, France*
[4]*CEA/DRECAM/SPAM, CEN Saclay, F-91105 Gif-sur-Yvette, France*
(Received 18 June 2003; published 4 May 2004)

We report the results of experimental and theoretical investigations of the two-color, two-photon ionization of Ar atoms, using femtosecond pulses of infrared laser radiation in combination with its extreme-ultraviolet harmonics. It is shown that the intensities of the photoelectron lines resulting from the absorption of photons from both fields strongly depend both on the respective phases of the fields and on atomic quantities such as the asymmetry parameter. These phases, which are notoriously difficult to measure, can be estimated by changing the polarization state of the laser radiation.

DOI: 10.1103/PhysRevA.69.051401 PACS number(s): 32.80.Rm, 32.80.Fb, 42.65.Ky

Photoionization measurements provide invaluable information on the structure of the electronic cloud of an atom or a molecule. The general features of photoionization, namely, the energy dependence, the angular distribution of the photoelectrons, and resonance effects, have been studied in great detail using mainly synchrotron radiation sources [1–3]. More specific investigations have been carried out by means of two-photon pump-probe experiments combining laser and synchrotron radiation [4,5]. Novel high-order harmonic generation (HHG) sources providing ultrashort extreme-ultraviolet (XUV) or x-ray pulses lasting a few femtoseconds [6] or less [7,8] will provide a deeper insight into the electronic relaxation processes and into the dynamics of photoionization [9]. Today, femtosecond XUV sources such as high-order harmonic radiation or the recent TESLA free-electron laser [10] are in the process of being developed and characterized. The number of pump-probe studies with these sources is therefore still rather limited and experiments often serve as a characterization tool for the sources themselves [7,8,11].

Electron spectra obtained from irradiation of a gas sample with harmonic emission, reflecting the harmonic intensity distribution, contain a series of lines separated by 2ω. The combination of the harmonic pulse with part of the fundamental infrared (IR) beam in the interaction chamber will give rise to additional lines, when the intensity of the dressing IR beam is high enough ($>10^{10}$ W/cm^2) [12] and when both pulses overlap in time and space (see Fig. 1). In the intensity ranges considered here, these so-called sidebands are the result of a two-photon ionization process, as the presence of the IR beam leads to an additional absorption or emission of one IR photon simultaneously with the absorption of the XUV photon. The intensity and shape of the sidebands depend strongly on the characteristics of the two femtosecond pulses [13] and can therefore be utilized to characterize the XUV pulses [11,14]. Since a given sideband is made up of contributions from two consecutive harmonics, the sideband intensity will depend on the phase difference between the two harmonics as well as on the angular momenta and the relative phases of the outgoing electrons [15,16]. The former property has been recently used to show that harmonics generated in argon were phase locked, indicating that the light was emitted as a train of attosecond pulses [7].

In this paper, we investigate experimentally and theoretically the influence of the state of polarization of the IR probe pulse (linear polarization with an angle relative to that of the XUV field and the degree of ellipticity) on the formation of the sidebands resulting from interfering amplitudes involving two harmonics. In the case of photoionization with linearly polarized photons, the ionization signal is independent of the harmonic phases and the variation of the angle between the two polarization vectors of the XUV and IR field allows us to determine the asymmetry parameter for the one-photon ionization process. On the other hand, the sideband intensity is very sensitive to the relative phase of two consecutive harmonics, when the ellipticity of the IR photon is changed. It is demonstrated that the controlled variation of the polarization states of the light can provide detailed information on the photoionization process, especially on the asymmetry parameter β describing the angular distribution of the electrons produced by absorbing the XUV photon, by measuring the angle integrated ionization signal.

The experimental conditions used for the present study have been described in detail elsewhere [17]. Briefly, XUV photons are produced by HHG in an Ar gas cell from an intense (1 mJ, 50 fs) IR laser (810 nm) running at 1 kHz repetition rate (see Fig. 2). The generated harmonics are focused into the acceptance volume of a magnetic bottle electron spectrometer (MBES) installed in an experimental chamber filled with a static pressure of about 10^{-4} mbar Ar gas. One-photon ionization of the Ar $3p$ shell (binding energy about 15.8 eV) by the harmonics leads to a series of equidistant lines in the photoelectron spectrum corresponding to the photoionization process by the 11th ($\sim$17 eV) up to the 25th harmonic ($\sim$38 eV). The observation of higher harmonics is limited by the reflectivity of the focusing gold mirror used in the experimental vacuum chamber. In the in-

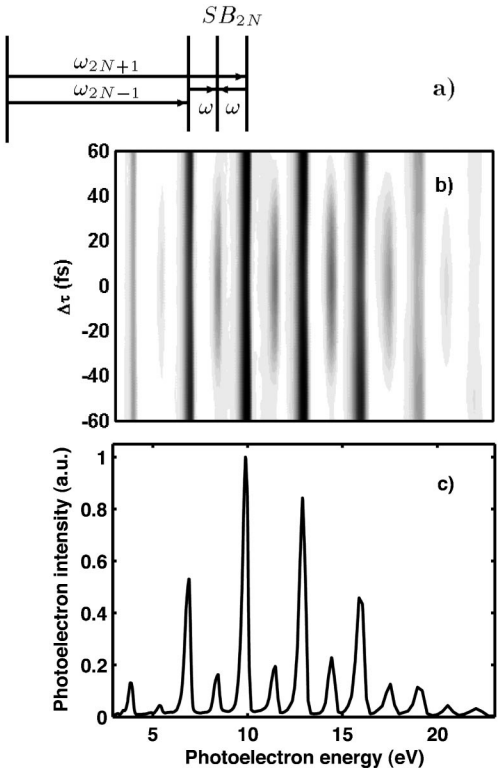

FIG. 1. (a) Scheme of the dominant photon absorption and emission processes involved in the generation of the sideband of order $2N$ ($2N\omega$ is the net amount of absorbed energy). (b) Photoelectron spectrum as a function of temporal delay $\Delta\tau$ between the XUV and the IR pulses. (c) Typical spectrum recorded at perfect temporal overlap between XUV and IR pulses ($\Delta\tau$=0 fs) with an IR beam intensity of about 5×10^{11} W/cm^2.

teraction region, the XUV beam intersects the IR probe beam (0.6 mJ) at an angle of about 8°. The spatial overlap between both beams and especially the size of the IR beam can be controlled by mechanical adjustment of a convex lens (f =50 cm). The temporal overlap is changed through an optical delay line introduced in the path of the beam used for HHG. In order to manipulate the polarization of the IR (probe) beam, a half-wave plate is installed just in front of the focusing lens, enabling us to change the relative angle Θ between the polarization vector of the IR and the harmonic beam. Alternatively, a quarter-wave plate allows us to vary the degree of ellipticity of the IR beam from linear to circular.

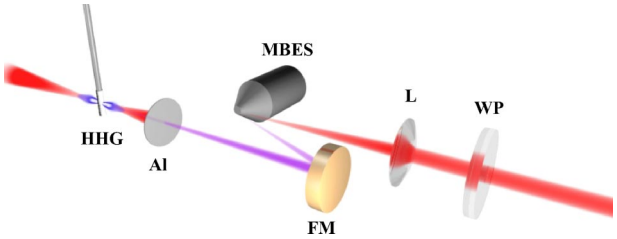

FIG. 2. (Color online) Schematic of the experimental setup. HHG, high harmonic generation; Al, Aluminum filter; MBES, Magnetic bottle electron spectrometer; WP, Retarding wave plate; L, Adjustable lens; FM, Gold focusing mirror.

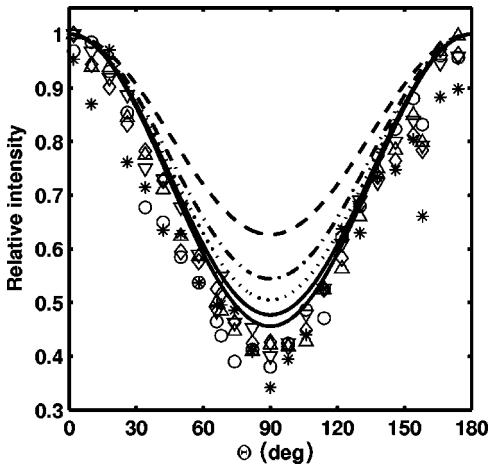

FIG. 3. Variation of the sideband intensity as a function of the relative angle Θ between the polarization vectors of the XUV and the IR beams. Experimental data for different sidebands: (*)SB_{14}, (◇)SB_{16}, (∇)SB_{18}, (Δ)SB_{20}, and (○)SB_{22}. Theoretical calculations: (--)SB_{14}, (-·)SB_{16}, (··)SB_{18}, (−)SB_{20}, and (−)SB_{22}.

A typical photoelectron spectrum is shown in Fig. 1(b) giving the photoelectron intensity as a function of electron kinetic energy (horizontal axis) and time delay between the two pulses (vertical axis). Figure 1(c) shows the spectrum obtained when both pulses are best temporally overlapped. The dominant structures in Fig. 1(b) are the vertical lines, which are not much affected by the presence of the IR pulses and which correspond to direct photoionization of Ar $3p$ electrons by the XUV photons. The spin-orbit splitting of about 0.18 eV between the $Ar^+3p^5\ ^2P_{1/2}$ and $^2P_{3/2}$ components [22] is not resolved in the present experiment. The sidebands show up for temporal delays $\Delta\tau$ between about −40 and +40 fs. The harmonic pulse durations, extracted from the combined knowledge of the energy-integrated sideband intensity profile and the independently measured 50 fs duration of the IR pulse, are found to be ≈30 fs, independent of the XUV photon energy. The shorter XUV pulse duration ensures that all atoms excited by XUV pulses are dressed by the same IR field at optimum spatial and temporal overlap.

When two linearly polarized photon beams are used, the intensity of the sidebands shows a strong and characteristic variation as a function of the relative angle Θ between both electrical field vectors (Fig. 3). Due to the 2π acceptance angle of the magnetic bottle analyzer, the intensity of the sidebands is independent of the precise shape of the angular distributions of the photoelectrons created in the two-photon process. The experimental results of Fig. 3 show a strong polarization dependence of the sideband intensity giving about 60% less intensity when the XUV and IR beams are crosspolarized (Θ=90°) compared to the case when they have the same direction of polarization (Θ=0°), as expected from simple classical arguments. In general, the observed variation is induced by a polarization dependent coupling between the intermediate (s or d) state and the final εp and εf continua. Furthermore, all sidebands seem to behave, within the experimental error, in the same way, indicating that the influence of the resonant $3s$-np excitations [18], which lie in the same photon energy region as the 17th and

19th harmonics, can be neglected for the present experiment.

The transition amplitude for the sideband denoted SB_{2N} is given by (atomic units are used, unless otherwise stated):

$$T_{2N}(n,l,m,\vec{k}) = T^{(+)}_{2N-1}(n,l,m,\vec{k})e^{-i(\phi_{2N-1}+\phi_L)} + T^{(-)}_{2N+1}(n,l,m,\vec{k})e^{-i(\phi_{2N+1}-\phi_L)}, \quad (1)$$

where (n,l,m) defines the initial state of the atom and $\vec{k}$ is the wave vector of the outgoing electron. ϕ_L, ϕ_{2N-1}, and ϕ_{2N+1} are the absolute phases of the fields of the IR laser and of the neighboring harmonics, respectively. $T^{(+)}$ ($T^{(-)}$) corresponds to the absorption (emission) of one laser photon. The fact that two quantum paths lead to the same final state gives rise to strong interferences.

In the soft-photon approximation, where the photon energy of the dressing laser is small against the harmonic XUV photons ($\omega_L \ll \omega_H$) and against the energy of the outgoing electrons ($\omega_L \ll k^2/2$) and where only low harmonic intensities are considered [19,20], the amplitudes are expressed as

$$T^{(\pm)}_{2N\mp1}(n,l,m,\vec{k}) = -i\pi \frac{\sqrt{I_H}}{\omega_{2N\mp1}} J_{\pm1}(\vec{\alpha}^{\pm}_L \cdot \vec{k}) T_1(n,l,m,\vec{k}), \quad (2)$$

where $\vec{\alpha}^{+}_L = \sqrt{I_L}/\omega^2_L \vec{\epsilon}_L$ for the absorption of one laser photon [$\vec{\alpha}^{-}_L = (\sqrt{I_L}/\omega^2_L)\vec{\epsilon}^{*}_L$ for emission], and $\vec{\epsilon}_H$ and $\vec{\epsilon}_L$ are the polarization vectors for the harmonic and laser field respectively. $T_1(n,l,m,\vec{k})$ represents the one-photon transition amplitude between the state (nlm) and a continuum state with energy $E_k = \frac{1}{2}k^2 = E_{nlm} + \omega_{2N-1} + \omega_L$. In the soft-photon approximation the energy of the intermediate state coincides with that of the final state. The effect of the laser field is entirely contained in the Bessel function $J_{\pm1}$ and the exchange of the laser photon appears through the factor $(\vec{\alpha}_L \cdot \vec{k})$. For moderate laser intensities, which is the case here, one can retain only the lowest-order term in the expansion of the Bessel function and the difference between the two amplitudes lies only in the term $(\vec{\epsilon}_L \cdot \vec{k})$ which becomes complex conjugate for $T^{(-)}$.

Finally, the angle-integrated sideband intensity, which is the relevant quantity for a comparison with the experimental data, is given as the average over the individual intensity $I_{2N}(n,l,m)$ for each magnetic sublevel m of the initial state:

$$I_{2N}(n,l,m) = \int d\Omega(\vec{k}) |T_{2N}(n,l,m,\vec{k})|^2. \quad (3)$$

Within the framework of the soft-photon approximation, the two-photon amplitudes are expressed in terms of known one-photon dipole matrix elements associated to the transition from the initial p state towards the s and d continua [21]. The "atomic phases" that enter the two-photon amplitudes [16] do not appear explicitly, although Eq. (2) involves a complex quantity due to the contributions of the s- and d-continuum phase shifts. We stress at this point that in contrast to one-photon ionization, the angle-integrated sideband intensities depend on these s and d phase shifts of the continuum wave functions.

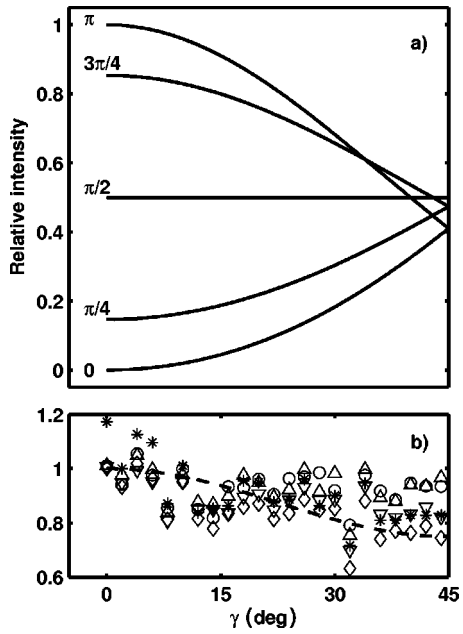

FIG. 4. Variation of sideband intensity as a function of the angle of rotation γ of the major axis of the ellipse described by the tip of the electric-field vector relative to the polarization direction of the XUV field. [The degree of ellipticity is $\tan(\gamma)$.] (a) Theoretical calculations for sideband 14 for different $\Delta\phi$. (b) Experimental data for different sidebands: (*)SB_{14}, ($\diamond$)SB_{16}, (∇)SB_{18} (Δ)SB_{20}, and ($\bigcirc$)SB_{22}. Broken line: theoretical calculation averaged over all $\Delta\phi$ for SB_{14}.

When both fields are linearly polarized, the harmonic phase and intensity dependence factorize and the normalized sideband intensity depends only on the angle between the two polarizations. One can show that when starting from a p state the sideband intensity is proportional to

$$I_{2N}(n,l=1,m) = 1 - \frac{3\beta(E_k)}{5+2\beta(E_k)} \sin^2\Theta, \quad (4)$$

where $\beta(E_k)$ is the usual one-photon asymmetry parameter [21]. The resulting theoretical curves, displayed in Fig. 3 as a function of Θ, are in good agreement with the experimental data regarding the general shape and the relative intensity variation. Only for the lowest sidebands some differences are observed, but, as indicated above, for these lines the soft-photon approximation is not applicable. A fit of the experimental data for the highest sideband with the above formula leads to asymmetry parameters equal to 1.7 ± 0.1, in reasonable agreement with other experimentally determined data [22] for this range of photon energy.

In the same way as for the case of two linearly polarized photons, we have also calculated the two-photon ionization probability as a function of ellipticity of the IR field (see Fig. 4). In this case, $\vec{\epsilon}_L$ is a complex vector and no factorization is possible. The amplitudes now depend on the state of polarization of the probe beam and can be expressed in a similar way as in Eq. (4), i.e.,

$$I_{2N}(n,l=1,m) = 1 - \cos\Delta\phi(\cos^4\gamma - \sin^4\gamma) + \frac{6\beta(E_k)}{5+2\beta(E_k)}\sin^2\gamma\cos^2\gamma(\sin\Delta\phi - 1), \quad (5)$$

where γ is defined as the angle of rotation of the major axis of the ellipse described by the tip of the electric-field vector relative to the polarization direction of the XUV field. [The degree of ellipticity is equal to $\tan(\gamma)$.] As a consequence the results are sensitive to the phase difference

$$\Delta\phi = 2\phi_L + \phi_{2N-1} - \phi_{2N+1}, \quad (6)$$

where $\phi_L = \omega\Delta\tau$ depends on the time delay $\Delta\tau$ between the two pulses. The theoretical results plotted in Fig. 4 as a function of the time delay strongly vary with $\Delta\phi$.

Experimentally, however, the finite XUV and IR beams intersect at a nonzero angle implying that all possible phase differences between the two beams are sampled throughout the interaction region imaged by the MBES. The resulting variation of the sideband intensity is given as a function of the angle of rotation, γ, in Fig. 4(b). The intensities of the sidebands are only weakly influenced by the degree of ellipticity and, again, the result does not depend on the sideband energy. An average calculated over all possible $\Delta\phi$ for different sideband orders, shown by the broken line in Fig. 4(b), accounts for this experimental feature. This curve is in qualitative agreement with the experimental data, but does not allow us to deduce the phase differences between subsequent harmonics.

On the basis of the present data, we conclude that the variation of the polarization state of the IR field with respect to the linearly polarized XUV field can provide information about the phase differences between consecutive harmonics as well as atomic quantities involving continuum states. Further experiments and calculations are certainly needed and the present experiments represent only a starting point for this type of measurement. Two-photon experiments combined with angular distribution measurements and the variation of polarization characteristics of the IR probe beam provide an ideal testing ground for exploring the internal dynamics of photoionization of field-dressed atoms. In this way, they are of fundamental interest for many experiments planned at the new femtosecond XUV and x-ray sources.

The authors acknowledge the support of the European Community (TMR-grant "Access to Large Scale Facilities," Contract No. HPRI-CT-1999-00041, RTD-project "X-Ray FEL Pump-Probe", Contract HRPI-CT-1999-50009, the ATTO network Grant No. HPRN-CT-2000-00133) and the Swedish Science Council.

[1] V. Schmidt, Rep. Prog. Phys. **55**, 1483 (1992).
[2] V. Schmidt, *Electron Spectrometry of Atoms using Synchrotron Radiation* (Cambridge University Press, Cambridge, 1997).
[3] G. B. Armen *et al.*, J. Phys. B **33**, R49 (2000).
[4] K. Godehusen *et al.*, Phys. Rev. A **58**, R3371 (1998).
[5] Ph. Wernet *et al.*, Phys. Rev. A **64**, 042707 (2001).
[6] T. Brabec and F. Krausz, Rev. Mod. Phys. **72**, 545 (2000).
[7] P. M. Paul *et al.*, Science **292**, 1689 (2001).
[8] M. Hentschel *et al.*, Nature (London) **414**, 509 (2001).
[9] M. Drescher *et al.*, Nature (London) **419**, 803 (2002).
[10] V. Ayvazyan *et al.*, Phys. Rev. Lett. **85**, 3825 (2002).
[11] J. Norin *et al.*, Phys. Rev. Lett. **88**, 193901 (2002).
[12] J. M. Schins *et al.*, Phys. Rev. Lett. **73**, 2180 (1994).
[13] T. E. Glover *et al.*, Phys. Rev. Lett. **76**, 2468 (1996).
[14] E. S. Toma *et al.*, Phys. Rev. A **62**, 061801 (2000).
[15] R. Taïeb *et al.*, Phys. Rev. A **62**, 013402 (2000).
[16] V. Véniard *et al.*, Phys. Rev. A **54**, 721 (1996).
[17] R. Lopez-Martens *et al.*, Eur. Phys. J. D **26**, 105 (2003).
[18] S. L. Sorensen *et al.*, Phys. Rev. A **50**, 1218 (1994).
[19] N. M. Kroll and K. M. Watson, Phys. Rev. A **8**, 804 (1973).
[20] A. Cionga *et al.*, Phys. Rev. A **47**, 1830 (1993).
[21] D. J. Kennedy and S. T. Manson, Phys. Rev. A **5**, 227 (1972).
[22] D. M. P. Holland *et al.*, Nucl. Instrum. Methods Phys. Res. **195**, 331 (1982).